Supporting Information for

Evaluation of Semiconducting Molecular Thin Films Solution-Processed via the Photoprecursor Approach: The Case of Hexyl-Substituted Thienoanthracenes

Cassandre Quinton,[a] Mitsuharu Suzuki,*[a] Yoshitaka Kaneshige,[a] Yuki Tatenaka,[ab] Chiho Katagiri,[c] Yuji Yamaguchi,[c] Daiki Kuzuhara,[a] Naoki Aratani,[a] Ken-ichi Nakayama,[cd] and Hiroko Yamada*[ad]

[a] *Graduate School of Materials Science, Nara Institute of Science and Technology (NAIST), 8916-5 Takayama-cho, Ikoma, Nara 630-0192, Japan*

[b] *Dojindo Laboratories, 2025-5 Tabaru, Mashiki-machi, Kumamoto 861-2202, Japan*

[c] *Department of Organic Device Engineering, Yamagata University, 4-3-16 Jonan, Yonezawa, Yamagata 992-8510, Japan*

[d] *Core Research for Evolutional Science and Technology (CREST), Japan Science and Technology Agency (JST), 4-1-8 Honcho, Kawaguchi, Saitama 332-0012, Japan*

Correspondence and requests for materials should be addressed to

H.Y. (hyamada@ms.naist.jp) or M.S. (msuzuki@ms.naist.jp)

Contents

1. Photoreactions in solution

The photoreactions of α-diketones **1** and **2** were monitored by NMR and UV–vis spectroscopy as follows: For the monitoring by NMR, approximately 1 mg of a photoprecursor was completely dissolved in 0.5 mL of $CDCl_3$ in an NMR tube equipped with a J. Young valve. The solution was degassed by three freeze–thaw cycles, and the tube was refilled with argon. The solution was irradiated with a metal-halide lamp through a blue cut filter, and subjected to ^{1}H NMR measurements every 40 s. Sample solutions for UV–vis measurements were prepared by dissolving approximately 0.2 mg of a photoprecursor in 10 mL of toluene. Each solution was transferred to a cuvette, before deoxygenated by argon bubbling for at least 30 min. The UV–vis absorption was measured periodically during the irradiation with a blue LED lamp. The results are shown in Figs. 4 and S1 for photoprecursors **1** and **2**, respectively.

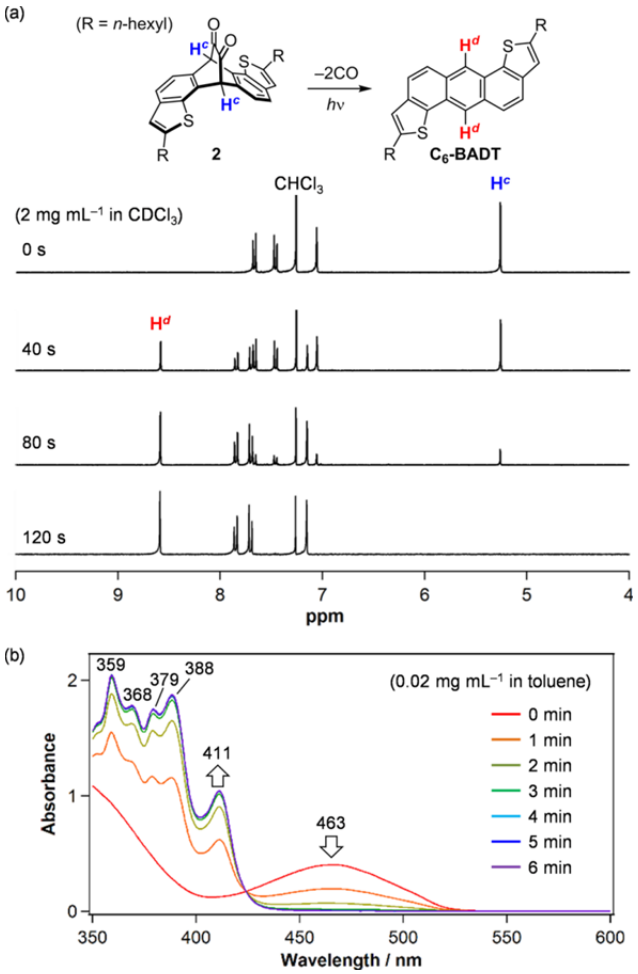

Fig. S1 Change in (a) NMR and (b) UV–vis spectra during the conversion of **2** to **C_6-BADT** under photoirradiation.

2. Photoelectron spectroscopy in air

The ionization energies of **C_6-ATT** and **C_6-BADT** thin films were measured on a Bunko Keiki AC-3 photoelectron spectroscopy instrument. The samples were prepared on ITO/glass substrates by either of (a) vacuum deposition of **C_6-ATT** or **C_6-BADT** with a deposition rate of 1.8 nm min^{-1}; (b) spin coating of a 10 mg mL^{-1} solution of **1** or **2** in chloroform at 800 rpm for 30 s followed by irradiation with a blue LED (λ = 460–490 nm) at 200 mW cm^{-2} for 30 min; or (c) direct spin coating of a 10 mg mL^{-1} solution of **C_6-ATT** or **C_6-BADT** in chlorobenzene/chloroform (1:1) at 800 rpm for 30 s. The spin coating and photoreaction were done in a nitrogen-filled glovebox. The obtained ionization energies (Figs. S2 and S3) are used as the approximate HOMO levels of the materials in the thin-film state for comparison purposes.

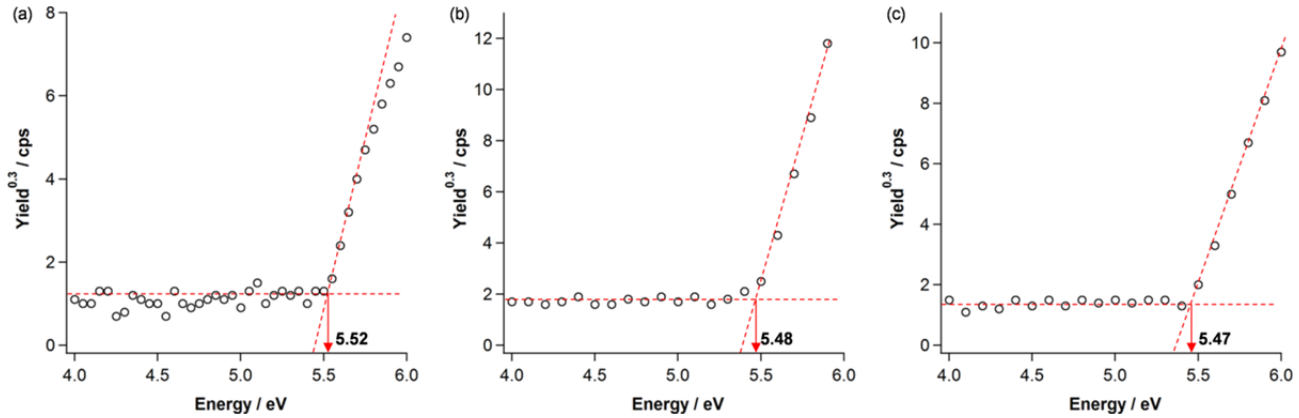

Fig. S2 Photoelectron spectra of **C_6-ATT** thin films prepared by (a) vacuum deposition, (b) photoprecursor approach, and (c) direct spin coating.

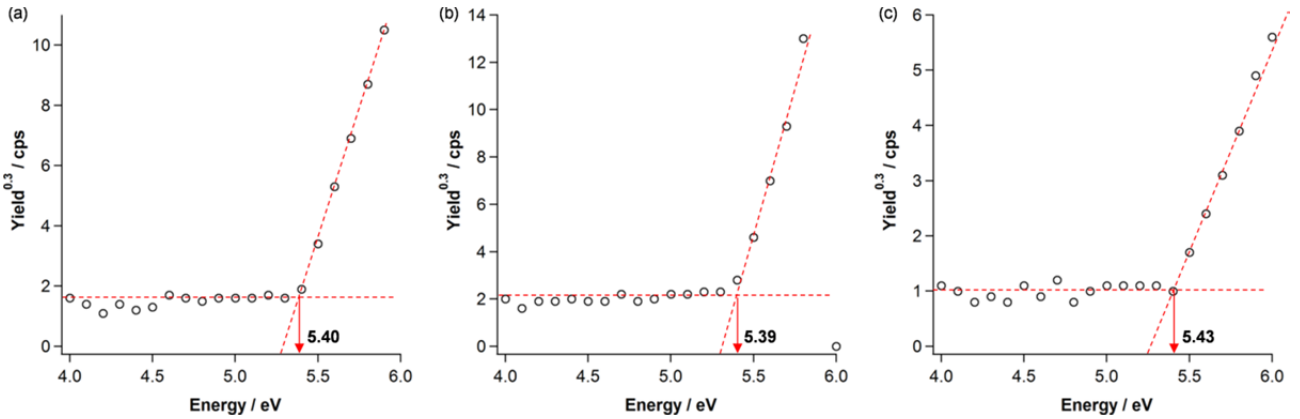

Fig. S3 Photoelectron spectra of **C_6-BADT** thin films prepared by (a) vacuum deposition, (b) photoprecursor approach, and (c) direct spin coating.

3. Cyclic voltammetry

The HOMO levels of **C_6-ATT** and **C_6-BADT** were also estimated from the onset of the first oxidation peak in cyclic voltammograms following the known empirical equation "HOMO = $-E^{ox}_{onset}$ – 4.8 eV", where E^{ox}_{onset} is referenced to the ferrocene/ferrocenium (Fc/Fc^+) standard.[S1] The estimated HOMO levels are –5.25 and –5.40 eV for **C_6-ATT** and **C_6-BADT**, respectively.

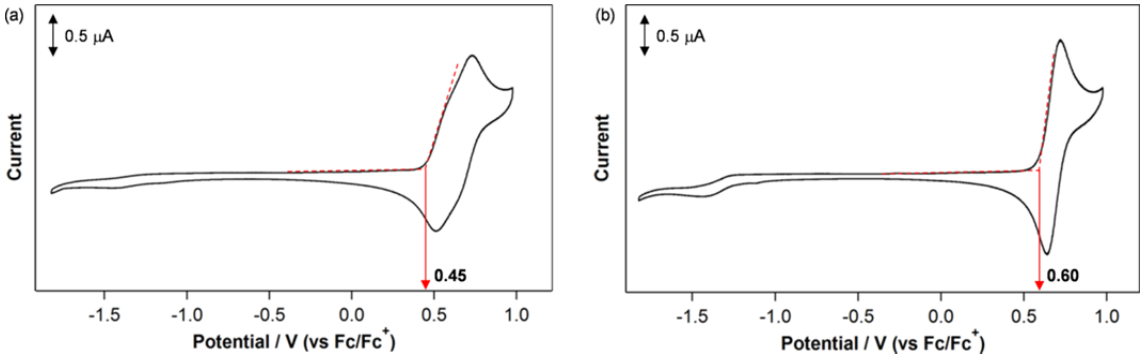

Fig. S4 Cyclic voltammograms of (a) **C_6-ATT** and (b) **C_6-BADT** in CH_2Cl_2 containing 0.1 M tetrabutylammonium hexafluorophosphate as support electrolyte. Reference electrode: $Ag/AgNO_3$, counter electrode: Pt wire, working electrode: glassy carbon (3 mmI.D.). Scan rate: 0.1 V s^{-1}.

[S1] Y. Liu, M. S. Liu and A. K.-Y. Jen, *Acta Polym.* **1999**, *50*, 105–108.

4. Density functional theory calculations

4.1. Method

All calculations were performed using the B3LYP method implemented in *Gaussian 09*, full citation of which is shown in the next section. Geometry optimizations were performed using the 6-31G(d) basis set with tight convergence criteria and no symmetry constraints. Vibrational frequencies were computed for all optimized structures to verify that these structures were minima. In these calculations, the hexyl groups of **C_6-ATT** and **C_6-BADT** were replaced with methyl (the resulting compounds are denoted as **Me-ATT** and **Me-BADT**, respectively) to save calculation time.

4.2. Full citation for Gaussian 09

Gaussian 09, Revision C.01: M. J. Frisch, G. W. Trucks, H. B. Schlegel, G. E. Scuseria, M. A. Robb, J. R. Cheeseman, G. Scalmani, V. Barone, B. Mennucci, G. A. Petersson, H. Nakatsuji, M. Caricato, X. Li, H. P. Hratchian, A. F. Izmaylov, J. Bloino, G. Zheng, J. L. Sonnenberg, M. Hada, M. Ehara, K. Toyota, R. Fukuda, J. Hasegawa, M. Ishida, T. Nakajima, Y. Honda, O. Kitao, H. Nakai, T. Vreven, J. A. Montgomery, Jr., J. E. Peralta, F. Ogliaro, M. Bearpark, J. J. Heyd, E. Brothers, K. N. Kudin, V. N. Staroverov, T. Keith, R. Kobayashi, J. Normand, K. Raghavachari, A. Rendell, J. C. Burant, S. S. Iyengar, J. Tomasi, M. Cossi, N. Rega, J. M. Millam, M. Klene, J. E. Knox, J. B. Cross, V. Bakken, C. Adamo, J. Jaramillo, R. Gomperts, R. E. Stratmann, O. Yazyev, A. J. Austin, R. Cammi, C. Pomelli, J. W. Ochterski, R. L. Martin, K. Morokuma, V. G. Zakrzewski, G. A. Voth, P. Salvador, J. J. Dannenberg, S. Dapprich, A. D. Daniels, O. Farkas, J. B. Foresman, J. V. Ortiz, J. Cioslowski, and D. J. Fox, Gaussian, Inc., Wallingford CT, 2010.

4.3. Cartesian coordinates of the optimized structures

Table S1 Cartesian coordinates of **Me-ATT** optimized at the B3LYP/6-31G(d). (Sum of electronic and zero-point energies = –2594.077725 Hartree; Number of imaginary frequencies = 0.)

Symbol	X	Y	Z
C	–3.71743	0.71875	0.00003
C	–3.71743	–0.71875	0.00001
C	–2.49558	–1.39076	0.00000
C	–1.22601	–0.72210	0.00001
C	–1.22601	0.72209	0.00003
C	–2.49558	1.39076	0.00003
C	0.00000	–1.39575	0.00001
C	1.22601	–0.72209	0.00001
C	1.22601	0.72210	0.00003
C	0.00000	1.39575	0.00004
C	2.49558	–1.39076	0.00001
C	3.71743	–0.71875	0.00002
C	3.71743	0.71875	0.00003
C	2.49558	1.39076	0.00004
C	4.83834	1.61380	0.00005
C	4.49089	2.93278	0.00007
S	2.74382	3.12757	0.00006
S	2.74382	–3.12757	–0.00002
C	4.49089	–2.93278	–0.00001
C	4.83834	–1.61380	0.00001
S	–2.74382	3.12757	0.00006

C	–4.49089	2.93278	0.00004
C	–4.83834	1.61380	0.00003
C	–4.83834	–1.61380	0.00000
C	–4.49089	–2.93278	–0.00001
S	–2.74382	–3.12757	–0.00002
C	5.39136	–4.13094	–0.00002
C	5.39136	4.13094	0.00009
C	–5.39136	4.13094	0.00005
C	–5.39136	–4.13094	–0.00001
H	0.00000	–2.48305	–0.00001
H	0.00000	2.48305	0.00005
H	5.87231	1.28399	0.00005
H	5.87231	–1.28399	0.00001
H	–5.87231	1.28399	0.00003
H	–5.87231	–1.28399	0.00000
H	5.23253	–4.76104	–0.88383
H	6.43740	–3.80891	–0.00001
H	5.23252	–4.76107	0.88377
H	6.43740	3.80892	0.00009
H	5.23253	4.76107	–0.88370
H	5.23252	4.76104	0.88389
H	–5.23253	4.76105	–0.88375
H	–6.43740	3.80891	0.00005
H	–5.23252	4.76105	0.88384
H	–6.43740	–3.80892	0.00000
H	–5.23253	–4.76105	–0.88381
H	–5.23252	–4.76106	0.88378

Table S2 Cartesian coordinates of **Me-BADT** optimized at the B3LYP/6-31G(d). (Sum of electronic and zero-point energies = –1566.707887 Hartree; Number of imaginary frequencies = 0.)

Symbol	X	Y	Z
C	2.81790	2.47599	0.00005
C	3.54855	1.24653	0.00006
C	2.85000	0.03606	0.00007
C	1.42148	–0.02777	0.00006
C	0.71238	1.23102	0.00004
C	1.45234	2.46130	0.00004
C	4.97192	1.05755	0.00008
C	5.35620	–0.25008	0.00009
C	0.68731	–1.21921	0.00006
C	–0.71238	–1.23102	0.00005
C	–1.42148	0.02777	0.00003
C	–0.68731	1.21921	0.00003
C	–1.45234	–2.46130	0.00005
C	–2.81790	–2.47599	0.00004
C	–3.54855	–1.24653	0.00002
C	–2.85000	–0.03606	0.00002
C	–4.97192	–1.05755	0.00001
C	–5.35620	0.25008	0.00000
S	–3.95862	1.32232	0.00000
S	3.95862	–1.32232	0.00009
H	3.36105	3.41740	0.00005
H	0.89372	3.39384	0.00003

H	5.68276	1.87846	0.00008
H	1.21325	–2.17149	0.00007
H	–1.21325	2.17149	0.00002
H	–0.89372	–3.39384	0.00006
H	–3.36105	–3.41740	0.00004
H	–5.68276	–1.87846	0.00001
C	6.74522	–0.81283	0.00010
H	6.93404	–1.43471	0.88390
H	6.93406	–1.43471	–0.88368
H	7.47549	0.00234	0.00011

4.4. Frontier-orbital energies

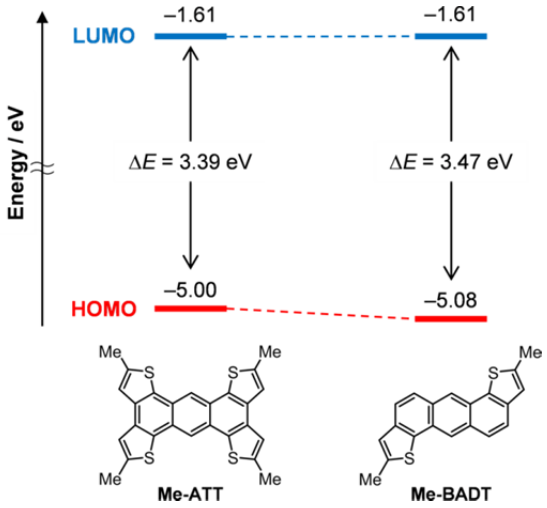

Fig. S5 Calculated frontier orbital energy levels of **Me-ATT** and **Me-BADT**, model compounds of **C_6-ATT** and **C_6-BADT**, respectively. Energies are shown in eV.

5. Simulated powder X-ray diffraction parameters

Powder X-ray diffraction patterns were simulated from the single-crystal X-ray structures[S2] using Mercury CSD 3.3 (Tables S3 and S4). Approximate molecular dimensions are also estimated from the crystal structures (Figs S6).

Table S3 Powder X-ray diffraction parameters simulated from the single-crystal X-ray structure of **C_6-ATT**.

h	*k*	*l*	*d*-spacing	F^2	multiplicity
0	0	2	16.0459	21068.2	2
1	0	–1	12.3491	10098.1	2
1	0	1	10.8969	2658.38	2
1	0	–3	8.95826	9.92816	2
0	0	4	8.02293	811.902	2
1	0	3	7.44244	222.338	2
2	0	0	6.19292	1989.84	2
1	0	–5	6.18599	1795.97	2
2	0	–2	6.17454	0.0978281	2
2	0	2	5.44843	48.0953	2
2	0	–4	5.41112	4611.72	2
0	0	6	5.34862	1233.58	2
1	0	5	5.3109	2714.73	2
0	1	1	4.82077	20052.8	4
0	1	2	4.66544	1590.89	4
1	0	–7	4.58484	1088.3	2
1	1	0	4.53716	1912.65	4
1	1	–1	4.53535	3895.52	4
2	0	4	4.51445	3212.71	2
2	0	–6	4.47913	38017.5	2
1	1	1	4.45081	12728.3	4
1	1	–2	4.44568	5684.57	4
0	1	3	4.43689	560.548	4
1	1	2	4.29041	59.0516	4
1	1	–3	4.28276	41.1579	4
3	0	–1	4.19438	37957.4	2
0	1	4	4.16687	216.594	4
3	0	–3	4.11636	17496.4	2
1	1	3	4.07866	68.4393	4
1	1	–4	4.06947	12.9609	4
1	0	7	4.06149	625.127	2
0	0	8	4.01147	415.323	2
3	0	1	4.00211	546.937	2
0	1	5	3.8827	1776.2	4
2	1	–1	3.85645	698.076	4
1	1	4	3.8393	8402.78	4
2	1	0	3.83109	1613.84	4
1	1	–5	3.82945	1783.05	4
2	1	–2	3.82673	1549.77	4
3	0	–5	3.80806	516.116	2
2	1	1	3.75378	5204.11	4

[S2] The structure of **C_6-ATT** was obtained in this work, and the structure of **C_6-BADT** was obtained from *J. Org. Chem.* **2009**, *74*, 4918–4926.

2	1	–3	3.74559	4623.43	4
2	0	6	3.72122	51.3555	2
2	0	–8	3.69351	2059.08	2
2	1	2	3.63348	915.451	4
3	0	3	3.63228	35.2291	2
2	1	–4	3.62235	56442.3	4
1	0	–9	3.60893	10062.2	2
0	1	6	3.60342	28.216	4
1	1	5	3.59182	3.51228	4
1	1	–6	3.58196	3076.76	4

Table S4 Powder X-ray diffraction parameters simulated from the single-crystal X-ray structure of **C_6-BADT**.

h	*k*	*l*	*d*-spacing	F^2	multiplicity
0	0	2	11.1068	182.158	2
1	0	0	7.91217	8722.12	2
0	1	1	6.70124	7478.59	4
1	0	–2	6.51247	1360.31	2
1	0	2	6.37808	1133.66	2
0	1	2	5.93933	1652.4	4
0	0	4	5.5534	1311.69	2
1	1	0	5.25475	217.752	4
1	1	–1	5.13049	971.809	4
0	1	3	5.09773	1969.87	4
1	1	1	5.09692	4457.71	4
1	1	–2	4.7771	2242.64	4
1	1	2	4.72329	1046.25	4
1	0	–4	4.5934	489.316	2
1	0	4	4.49907	2213.93	2
0	1	4	4.35743	985.599	4
1	1	–3	4.31525	1824.23	4
1	1	3	4.25598	4607.53	4
2	0	0	3.95609	106.003	2
1	1	–4	3.84511	4106.77	4
1	1	4	3.78927	2503.96	4
0	1	5	3.75542	0.101787	4
2	0	–2	3.753	2323.81	2
0	0	6	3.70227	298.676	2
2	0	2	3.70102	60299.2	2

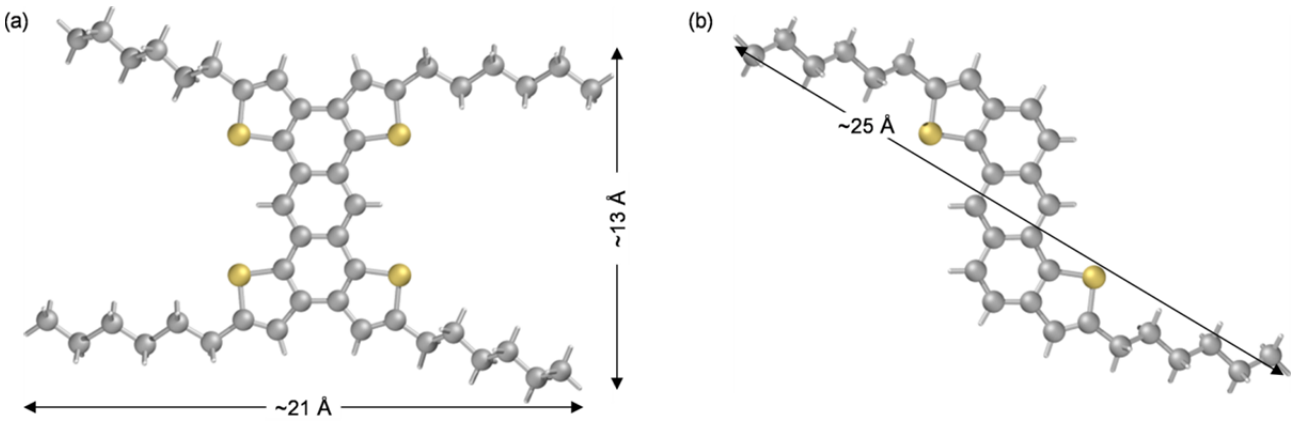

Fig. S6 Approximate molecular dimensions of (a) **C_6-ATT** and (b) **C_6-BADT** in the single-crystalline state.

6. Space-charge-limited-current measurements

Charge-carrier mobilities in **C_6-ATT** films were evaluated by the space-charge-limited-current (SCLC) method using an Agilent HP4155C semiconductor parameter analyzer. The sample prepared by either vacuum deposition or photoprecursor approach.

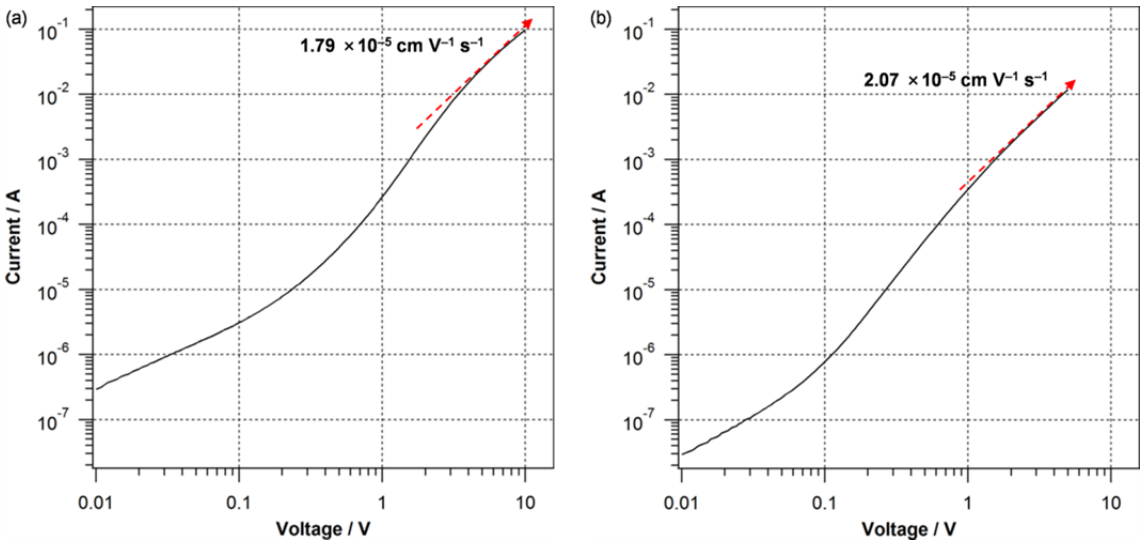

Fig. S7 Space-charge-limited-current (SCLC) measurements for **C_6-ATT** films prepared by (a) vacuum deposition (film thickness = 58.4 nm) and (b) photoprecursor approach (77.5 nm). The general device structure is [ITO/MoO_3 (5 nm)/**C_6-ATT**/MoO_3 (5 nm)/Al (80 nm)], and the device area is 2 × 2 mm^2.

7. AMF images of photoprecursor films

The surface morphology of the films of compound **1** and **2** were probed by AFM. They are very smooth and homogeneous associated with small RMS values of surface roughness. The samples were prepared by spin coating of a 10 mg ml^{-1} solution in chloroform at a rate of 800 rpm for 30 s.

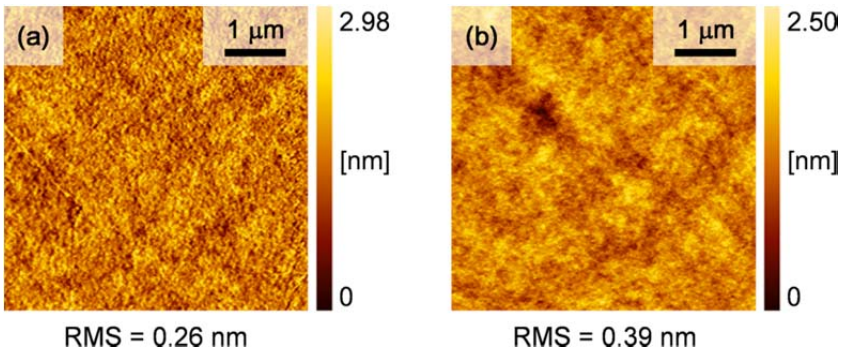

Fig. S8 Surface morphology of thin films of (a) compound **1** and (b) compound **2** observed by AFM in the tapping mode.

8. NMR spectra of photoprecursors 1 and 2

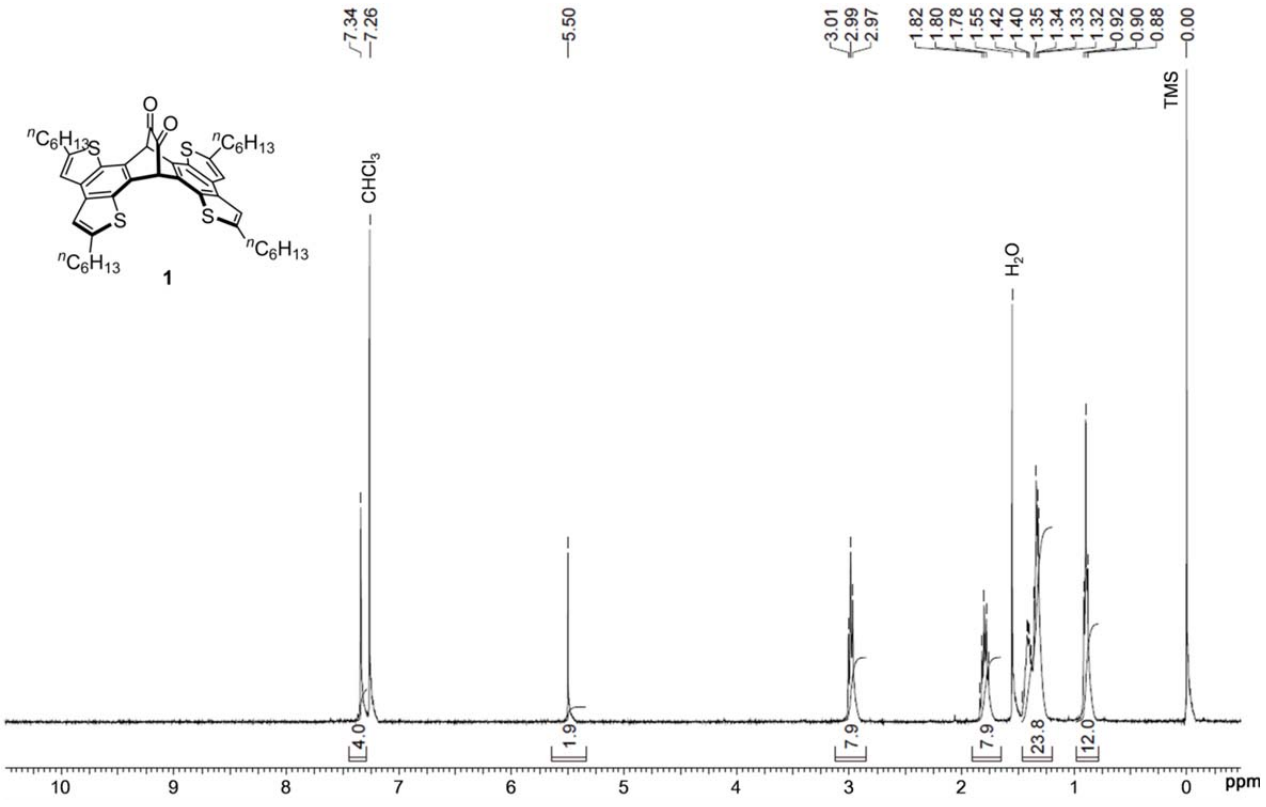

Figure S8. ^{1}H NMR of photoprecursor **1** ($CDCl_3$, 300 MHz).

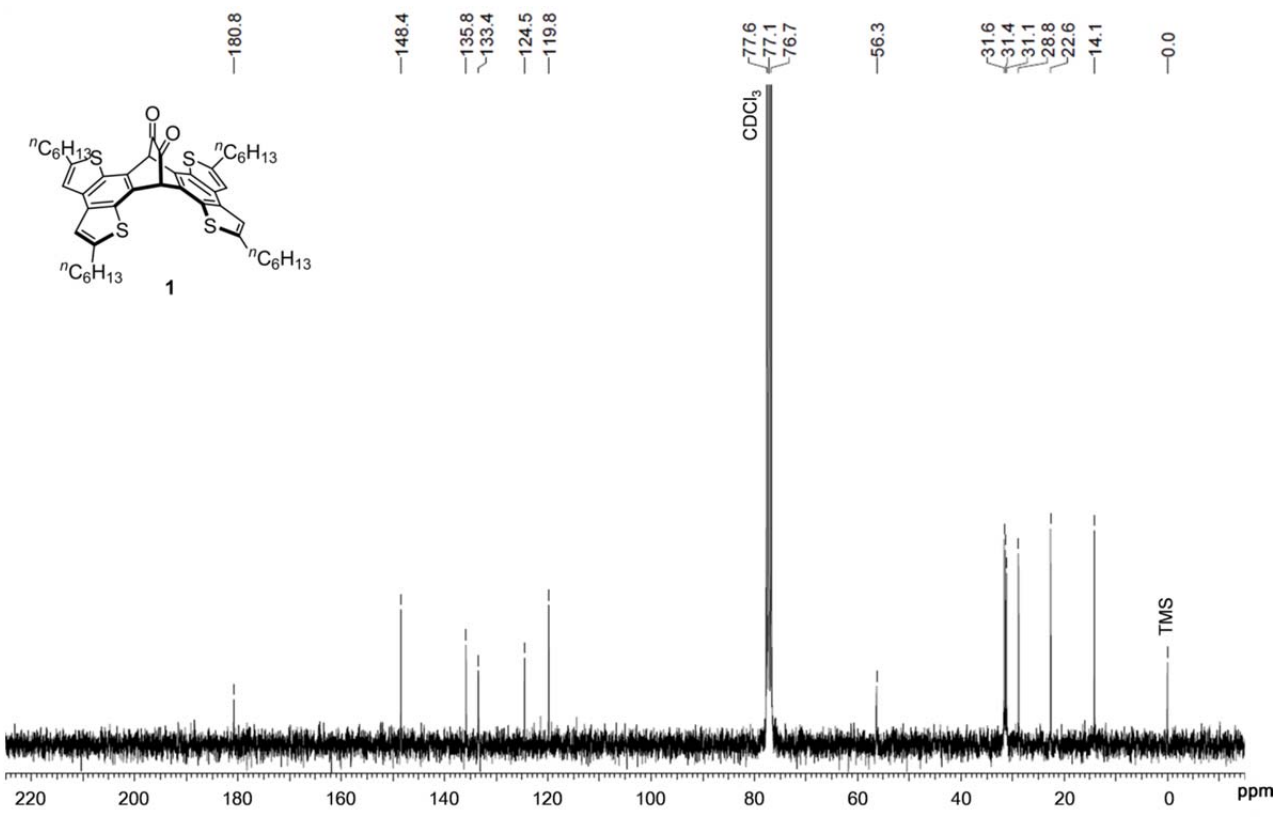

Figure S9. ^{13}C NMR of photoprecursor **1** ($CDCl_3$, 75 MHz).

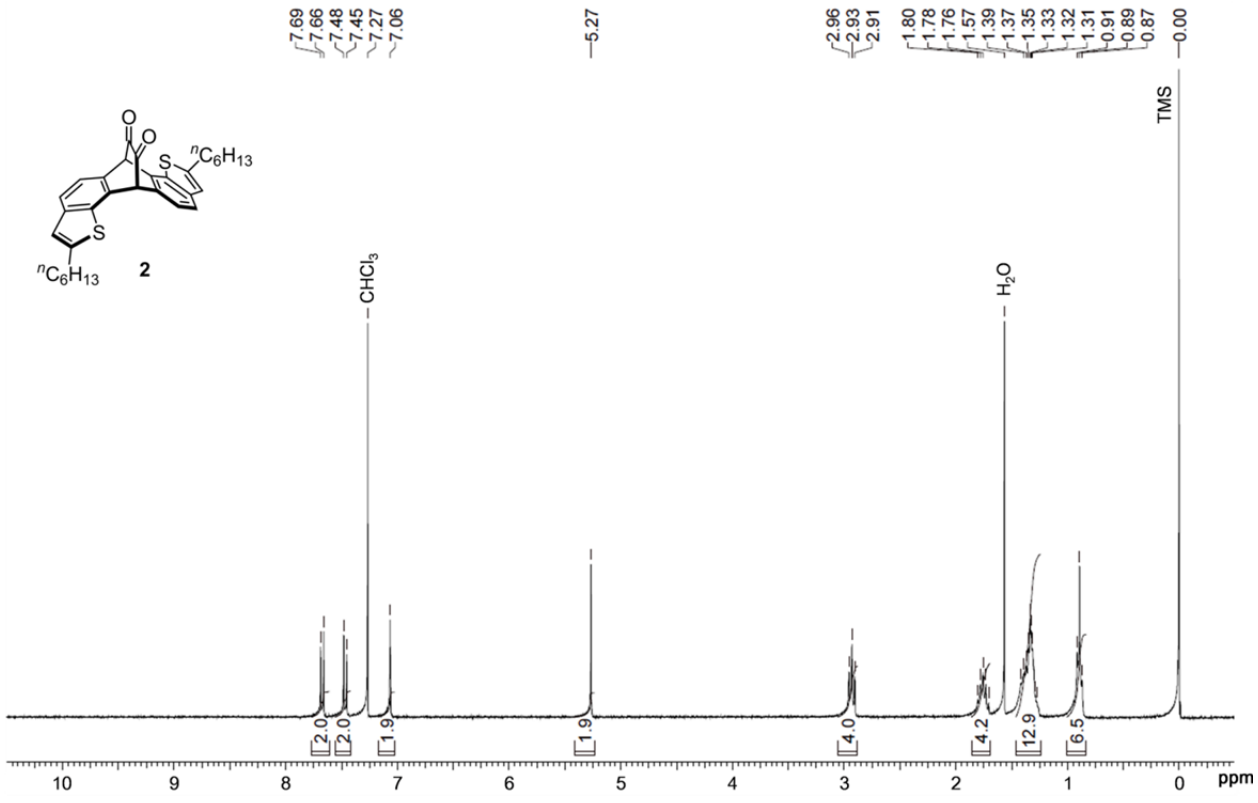

Figure S10. ^{1}H NMR of photoprecursor **2** ($CDCl_3$, 300 MHz).

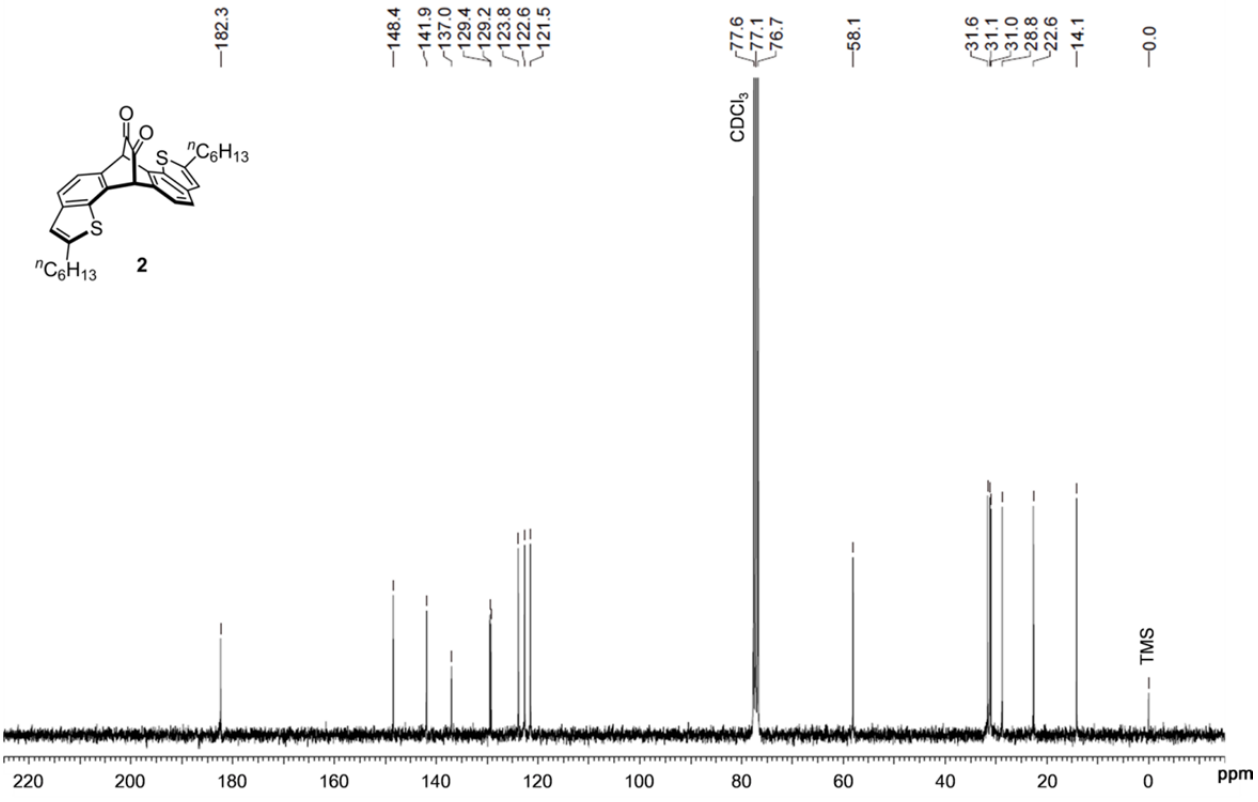

Figure S11. ^{13}C NMR of photoprecursor **2** ($CDCl_3$, 75 MHz).